Atmos. Chem. Phys. Discuss., 9, 24669–24715, 2009
www.atmos-chem-phys-discuss.net/9/24669/2009/

Atmospheric
Chemistry
and Physics
Discussions

Surfactants in cloud droplet activation: mixed organic-inorganic particles

N. L. Prisle[1], T. Raatikainen[2], A. Laaksonen[3], and M. Bilde[1]

[1]University of Copenhagen, Department of Chemistry, Universitetsparken 5, 2100, Copenhagen, Denmark
[2]Finnish Meteorological Institute, Erik Palmenin Aukio 1, 00101, Helsinki, Finland
[3]University of Kuopio, Department of Physics, P.O. Box 1627, 70211, Kuopio, Finland

Received: 13 October 2009 – Accepted: 26 October 2009 – Published: 18 November 2009

Correspondence to: N. L. Prisle (nlp@kemi.ku.dk)

Published by Copernicus Publications on behalf of the European Geosciences Union.

Abstract

Organic compounds with surfactant properties are commonly found in atmospheric aerosol particles. Surface activity can significantly influence the cloud droplet forming ability of these particles. We have studied the cloud droplet formation by two-component particles comprising one of the organic surfactants sodium octanoate, sodium decanoate, sodium dodecanoate, and sodium dodecyl sulfate, mixed with sodium chloride. Critical supersaturations were measured with a static diffusion cloud condensation nucleus counter (Wyoming CCNC-100B). Results were modeled from Köhler theory applying three different representations of surfactant properties: (1) using concentration-dependent surface tension reduction during droplet growth and explicitly accounting for surfactant surface partitioning in both solute suppression (Raoult effect) and curvature enhancement (Kelvin effect) contributions to the droplet equilibrium water vapor supersaturation, (2) disregarding surfactant partitioning and using a concentration-dependent surface tension for the droplets corresponding to a macroscopic (bulk) aqueous solution of the same overall composition, and (3) disregarding surfactant properties and assuming the constant surface tension of pure water throughout droplet activation. We confirm previous results for single-component organic surfactant particles, that experimental critical supersaturations are greatly underpredicted, if reduced surface tension is applied in Köhler theory while ignoring the effects of surface partitioning in droplets. We further show that assuming the constant surface tension of pure water can also lead to significant underpredictions of experimental critical supersaturations. The full account for surfactant partitioning in activating droplets generally predicts experimental critical supersaturations well. In addition, for mixed particles comprising less than 50% by mass of surfactant, ignoring surfactant properties and simply using the constant surface tension of pure water also provides a good first-order approximation of the observed activation.

1 Introduction

The influence of atmospheric aerosol particles on cloud formation and properties constitutes the single largest uncertainty in assessing anthropogenic climate forcing (IPCC, 2007). Cloud droplets form when water vapor condenses onto particle surfaces. In the process, particle constituents may dissolve into the aqueous phase and form solution droplets. The ability of particles to act as cloud condensation nuclei (CCN) therefore depends on their chemical composition, as well as size. Surface active molecules, or surfactants, concentrate in the surface and can reduce the surface tension of an aqueous solution. Reduced surface tension, compared to that of pure water, has been demonstrated in bulk samples of atmospheric cloud and fog water (Facchini et al., 1999, 2000) and in aqueous extracts of collected atmospheric aerosol samples from a wide variety of sources and environments, including biomass (Asa-Awuku et al., 2008) and coal burning (Oros and Simoneit, 2000), and marine (Mochida et al., 2002), rural (Kiss et al., 2005), and polluted environments (Dinar et al., 2006). The goal of this work is to advance the fundamental understanding of the role of surfactants in cloud microphysics, which is essential for proper representations of aerosol effects in atmospheric models.

Fatty acids and their salts constitute an important class of atmospheric surfactants and have been identified in aerosol samples from both marine (Mochida et al., 2003), urban (Yassaa et al., 2001), and continental (Cheng et al., 2004) environments. We have previously addressed the cloud microphysics of single-component particles comprising a series of saturated fatty acid sodium salts and demonstrated the importance of a comprehensive account for surfactant properties in predictions of cloud droplet formation (Prisle et al., 2008). Atmospheric particles are however generally mixtures of both organic and inorganic species (Murphy et al., 2006). Inorganic salts can directly influence organic surfactant properties and may also affect the relative importance of different surfactant properties for cloud droplet formation. In this work, we therefore take the next step and investigate two-component particles comprising organic surfactants mixed with sodium chloride (NaCl). Specifically, we have studied the sodium salts of n-octanoic (caprylic), n-decanoic (capric) and n-dodecanoic (lauric) acid. In addition, we included sodium dodecyl sulfate (SDS), which is a strong industrial surfactant with well-quantified properties. SDS has previously been targeted as a model compound for water-soluble atmospheric surfactants in cloud droplet formation studies of both single-component particles (Li et al., 1998; Sorjamaa et al., 2004) and mixed particles together with NaCl (Rood and Williams, 2001).

The fatty acid salts (FAS) and SDS are amphiphiles. Each molecular structure is characterized by a polar head-group (the $-\mathrm{COO}^-$ or $-\mathrm{SO}_4^-$ functional groups) and a non-polar unbranched hydrocarbon tail. To reduce destabilizing interactions with the polar water molecules in the aqueous phase, the surfactant molecules preferentially accumulate at the air-water interface and arrange themselves with the hydrophilic ends dissolved in the aqueous solution and the hydrophobic tails pointing outwards to the air. This is the origin of their surface activity.

The small solution droplets involved in cloud droplet formation typically have submicrometer diameters, whereas the overall dimensions of the bulk solutions characterized by conventional laboratory methods (as in surface tension measurements) or collected in field samples (like a bucket of rain water) are inherently much larger. We here follow the convention used in our previous study and denote bulk aqueous solutions as “macroscopic”, to comply with the “microscopic” droplets (Prisle et al., 2008). The term “bulk” designates the distinct bulk phase within an aqueous surfactant solution, to distinguish it from the surface phase. A similar practice is used by Ruehl et al. (2009).

When the surfactant molecules accumulate at the air-water interface of an aqueous solution, a non-uniform distribution arises, in terms of a concentration gradient between the solution bulk and surface phases. The relative distribution of surfactant molecules between these distinct phases is what we refer to as the surfactant (bulk-)surface partitioning. Due to surface partitioning, the relative dimensions of the bulk and surface phases become key factors in determining surfactant solution properties. Microscopic droplets have much larger surface-area-to-bulk-volume ratios than macroscopic solutions. At the surface-partitioning equilibrium, the relative distribution of surfactant molecules between the bulk and surface phases will therefore be different in microscopic droplets and in macroscopic solutions of the same total surfactant concentration. A comprehensive thermodynamic model of cloud droplet formation must therfore take surfactant surface partitioning in the droplets accordingly into account.

Here, we compare experimental observations of cloud droplet formation by mixed surfactant-NaCl particles to thermodynamic model predictions using three different representations of surfactant properties. We show that the cloud droplet forming potential is in all cases greatly overestimated by including reduced droplet surface tension while neglecting surfactant surface partitioning within the droplets. This confirms our previous results for pure-component particles comprising the same organic surfactants (Sorjamaa et al., 2004; Prisle et al., 2008). We furthermore show that, even assuming the constant surface tension of pure water can also lead to significant overestimations of the cloud droplet forming potential, if surfactant surface partitioning is not considered. A full account of surfactant properties, including surface partitioning, describes observations well. However, for mixed particles comprising less than about 50% by mass of surfactant, disregarding surfactant properties altogether also appears to be a good first-order approximation for describing cloud microphysics.

2 Experimental

We have measured the critical supersaturation as a function of dry particle diameter for two-component laboratory-generated particles comprising organic surfactant (SFT) and sodium chloride (NaCl) in different relative amounts. Particle compositions included one of the surfactants sodium octanoate ($CH_3(CH_2)_6COONa$; C8), sodium decanoate ($CH_3(CH_2)_8COONa$; C10), sodium dodecanoate ($CH_3(CH_2)_{10}COONa$; C12), and sodium dodecyl sulfate ($CH_3(CH_2)_{10}SO_4Na$; SDS), mixed with NaCl. Chemicals were obtained at the highest purities available from commercial sources: sodium octanoate (Sigma, capillary GC, minimum 99%), sodium decanoate (Fluka, purum. 98%), sodium dodecanoate (Sigma, Sigma Grade 99–100%), sodium dodecyl sulfate (Sigma, >99%), and sodium chloride (Riedel-deHaën, >99.8%). Before use, chemicals were baked overnight at moderate temperatures (<80°C) to evaporate any volatile impurities.

2.1 CCN measurements

Critical supersaturations were determined using a static thermal-gradient diffusion-type cloud condensation nucleus counter (Wyoming CCNC-100B) (Snider et al., 2006). The experimental set-up and procedures employed are described in detail by Prisle et al. (2008) (and references herein).

Particles were generated by atomization of aqueous solutions using a constant output atomizer (TSI-3076), operated in recirculation mode. The wet aerosol produced was subsequently dried by passing through a set of two silica-gel containing diffusion driers in series, followed by dilution with dry air. The relative humidity (RH) in the dry aerosol flow was typically between 5–8%, except for one occasion where the RH during one measurement (about 1.5 h) increased to nearly 20%. It is an underlying assumption that the relative mass fractions of organic-to-inorganic components in the dry particles reflect the solute composition in the atomizer solution. Atomizer solutions were prepared with de-ionized and purified water (18.2 MΩ cm resistivity, produced in a Milli-Q Plus Ultra Pure Water System). Total concentrations were between 0.12–0.31 g L^{-1}. Particle compositions studied comprised the FAS in approximate mass fractions of 20, 50, 80, and 95%, and SDS in approximate mass fractions of 20, 50, and 80%, relative to NaCl. Exact surfactant mass-fractions (w_{SFT} [%]) in the dried particles are given in Table 1.

From the produced polydisperse aerosol, a narrow electrical-mobility particle size-fraction was selected with an electrostatic classifier (TSI-3080). The number concentration of activated particles (CCN [cm^{-1}]) at selected water vapor supersaturations (SS [%]) was measured with the CCNC. The total particle number concentration (CN [cm^{-1}]) was measured in parallel using a condensation particle counter (TSI-3010). Selected particle electrical mobility diameters (D_p) were between 25–140 nm and CCNC supersaturations were in the range 0.2–2.0%. Purified and dried high-pressure air was used in all experiments. Laboratory temperatures were kept constant during the course of each experiment by a thermostat air-conditioning system and were in the range 296–297 K.

2.1.1 CCNC calibration and data fitting

The CCN experiments give the fraction of activated particles (CCN/CN) with a selected mobility diameter as a function of the supersaturation (SS) the particles were exposed to. These data were fitted with a four-parameter sigmoidal function $y=y_0+a/[1+\exp(-(x-x_0)/b)]$ (Prisle et al., 2008). Including correction for the doubly-charged particles simultaneously selected in the classifier, the experimental critical supersaturation (SS_c^{exp} [%]) was determined from the midpoint of the single-charged particles activation step (x_0 [%]). The CCNC supersaturation was calibrated with a linear relation, obtained from measurements on monodisperse ammonium sulfate ($(NH_4)_2SO_4$) and NaCl particles (Bilde and Svenningsson, 2004), such that $SS_c^{\text{exp}} = 0.6638\, x_0 - 0.01168$. Error bars depicted for the experimental critical supersaturations below are estimated as the 95%-confidence intervals corresponding to $\pm 2\tau$, where τ is the combined standard deviation from the sigmoidal fit to activated fractions and the linear supersaturation calibration (Prisle, 2006).

3 Theory

3.1 Köhler theory

Cloud droplet formation can be described by Köhler theory (Köhler, 1936) in terms of the equilibrium growth and activation of an aqueous solution droplet. The Köhler equation relates the equilibrium water vapor saturation ratio (S) over a spherical solution droplet to its diameter (d):

$$S \equiv \frac{p_w}{p_w^0} = a_w \exp\left(\frac{4 v_w \sigma}{RT d}\right) \tag{1}$$

where p_w is the equilibrium partial pressure of water over the solution droplet, p_w^0 is the saturation vapor pressure over a flat surface of pure water, a_w is the droplet solution water activity, v_w is the partial molar volume of water in the solution, σ is the droplet solution surface tension, R is the universal gas constant and T is the Kelvin temperature. We approximate v_w with the molar volume of pure water, given by the water molar mass and mass density as $v_w^0 = M_w/\rho_w$.

The water activity (a_w) term in Eq. (1) is equivalently called the Raoult term and describes how the equilibrium partial pressure of water over an aqueous solution is suppressed from the pure water saturation vapor pressure by dissolved solutes according to (the extended) Raoult's Law, $p_w = a_w p_w^0$. The exponential, or Kelvin, term of Eq. (1) accounts for the vapor pressure enhancement over a curved droplet surface by the Kelvin effect. The magnitude of the Kelvin term for a given droplet size (d) and corresponding surface curvature depends explicitly on the droplet solution surface tension (σ).

A plot of water saturation ratio (S) versus droplet diameter (d) gives the Köhler curve for the droplet and its maximum defines the critical saturation ratio (S_c) and the corresponding critical droplet diameter (d_c). Droplets that have been exposed to ambient saturation ratios larger than their threshold values ($S \geq S_c$) and surpassed their critical diameters ($d \geq d_c$) are assumed to be activated cloud droplets that will continue to grow into full-sized cloud drops, only limited by the transport of water vapor to the droplet surface. For convenience, we often refer to the water vapor supersaturations, $SS/[100\%] \equiv S - 1$, and analogously to the droplet critical supersaturations (SS_c [%]).

3.2 Surfactant surface partitioning

Surfactants (surface active molecules) preferentially concentrate at the air-water interface of aqueous solutions. The resulting (bulk-)surface partitioning of surfactant molecules can be thought of as governed by some equilibrium constant, $K_p \propto \partial\Gamma/\partial c^B$, where Γ (the surface excess) is the number of surfactant molecules per unit area in the surface phase (superscript S in the following) and c^B is the surfactant concentration per unit volume in the bulk phase (superscript B). The relative bulk-surface distribution of surfactant solute thus depends on its propensity for the surface phase (directly from the value of K_p) and on the relative dimensions of the solution bulk and surface phases (due to the implicit dependence of K_p on surface area and bulk volume). The latter can thus be expressed by the surface-area-to-bulk-volume ratio (A/V [μm^{-1}]) for the solution. For spherical liquid droplets with diameters of $d = 0.1,\ 1,$ and 10 μm, $A/V (= 6/d)$ is $60,\ 6,$ and 0.6 μm^{-1}, respectively, and for macroscopic solutions with flat surfaces, $A/V \rightarrow 0$ as $d \rightarrow \infty$.

At the (bulk-)surface partitioning equilibrium, properties of an aqueous surfactant solution, such as water activity (a_w) and surface tension (σ), are thermodynamically expressed as functions of the bulk phase composition (c^B). However, surface partitioning depletes the solution bulk phase of surfactant molecules and decreases c^B. Given the same total surfactant concentration per unit of total solution volume (c^T), the larger A/V of microscopic activating droplets entails that a larger fraction of the total number (n^T) of surfactant molecules in solution will reside in the surface (n^S) and a smaller fraction in the bulk phase (n^B) of the droplets, compared to macroscopic solutions. The change in bulk-composition from the overall solution composition due to surfactant surface partitioning is negligible in macroscopic solutions ($c^B \sim c^T$). For microscopic droplets, the bulk phase depletion of surfactant can, on the other hand, be significant ($c^B \ll c^T$). The resulting aqueous solution properties for a given overall composition, particularly the solute suppression of equilibrium water partial pressure and the surface tension reduction, will therefore depend on the solution A/V, determining the extent of surfactant depletion from the bulk phase due to surface partitioning.

Surfactant surface partitioning in microscopic droplets thus potentially affects cloud droplet activation through both Raoult and Kelvin effects. The smaller surfactant bulk phase concentration in a microscopic droplet, compared to a macroscopic solution with the same total concentration of dissolved surfactant (c^T), will be reflected in a diminished water partial pressure suppression by the Raoult effect (a larger water activity a_w) and a diminished surface tension reduction (a larger surface tension σ). The latter leads to an amplified curvature enhancement of water vapor pressure by the Kelvin effect, compared to a droplet of the same size (d), but with the surface tension of a macroscopic solution of the same total concentration. A simple illustration of the effect of surface partitioning on surfactant bulk-concentration and surface tension in droplets of different sizes is given in Appendix A.

4 Thermodynamic model

The thermodynamic model used in this work has been described in detail by Sorjamaa et al. (2004) and Prisle et al. (2008). All model calculations are based on evaluating the water vapor equilibrium saturation ratio (S) as a function of droplet diameter (d) from Eq. (1), for aqueous solution droplets with known initial sizes and compositions.

Droplets are assumed to form on spherical dry particles of known diameters and compositions. Dry particle diameters (D_p) correspond to the electrical-mobility diameter mode (D_p) selected in the CCN experiments and the compositions are analogously given by the respective surfactant (SFT) and NaCl mass fractions (w_{SFT} and w_{NaCl}, where $w_{\mathrm{SFT}}+w_{\mathrm{NaCl}}=1$). The total amounts of surfactant and NaCl solute (n^T_{SFT} [mol] and n^T_{NaCl} [mol]) in the droplets are then calculated from the dry particle volume (V_p) and mass fractions, assuming volume additivity of the components. Unit mass density is assumed for the fatty acid salts (FAS) ($\rho_{\mathrm{FAS}} = 1\ \mathrm{g\ cm^{-3}}$), owing to lack of bulk-density information for the solid FAS in general and for the mixed FAS–NaCl dry particles in particular. At a given droplet size, the total amount of water (n^T_w [mol]) is calculated from the volume of water, determined as the difference between the droplet and dry particle volumes ($V_w = V - V_p$), using the pure water molar volume, $n_w^T = V_w / v_w^0$.

Both surfactant and NaCl solutes are assumed to be completely dissolved in the droplet solution, that is, effects of limited water solubilities in macroscopic solutions on the concentration of dissolved particle constituents are not accounted for. It is furthermore assumed that dissolved surfactant and NaCl are fully dissociated, such that dissociation factors for both solute species are $\delta_{\mathrm{SFT}} = \delta_{\mathrm{NaCl}} = 2$. The applicability of these simplifying assumptions for the model calculations has been discussed in our previous work (Prisle et al., 2008). Physical properties of the surfactants and NaCl used in the calculations are summarized in Table 2.

For each droplet size and corresponding overall composition, the droplet bulk-composition is then determined. When surfactant surface partitioning in the droplet is not considered, the droplet bulk phase concentrations of water (c_w^B), surfactant (c_{SFT}^B), and NaCl (c_{NaCl}^B) are all set equal to the corresponding total droplet concentrations (c_w^T, c_{SFT}^T, and c_{NaCl}^T). Taking surface partitioning into account, these bulk phase concentrations are evaluated by solving the bulk-surface partitioning equilibrium for the droplets, as described in Sect. 4.1 below. Because activity data are to our knowledge not available, droplet solutions are treated as ideal by using bulk phase concentrations (on the scales of the respective reference states) instead of the appropriate activities for all droplet components. Particularly, the droplet bulk phase water activity is set equal to the corresponding water mole-fraction concentration ($a_w^B = x_w^B$). Droplet solution ideality is also implicitly assumed by some of the other approximations applied in these calculations. In most cases, droplets are sufficiently dilute at the point of activation that ideality of all droplet components must be a reasonable assumption (Prisle et al., 2008).

The water equilibrium saturation ratio (S) is then calculated for each droplet size (d) from Eq. (1). Droplet solution surface tension is either evaluated from a concentration-dependent ternary SFT-NaCl aqueous solution parametrization, $\sigma = \sigma(c_{\mathrm{SFT}}^B, c_{\mathrm{NaCl}}^B)$, or set equal to the constant value for pure water ($\sigma = \sigma_w$). Specifically, Köhler model predictions are made with three different representations of surfactant properties: (1) using a concentration-dependent droplet surface tension and explicitly accounting for the surfactant bulk-surface partitioning equilibrium in the droplets upon evaluation of both Raoult and Kelvin terms of Eq. (1), denoted "σ,p", (2) using a concentration-dependent droplet surface tension, but neglecting the effects of surfactant surface partitioning in the droplets and evaluating both Raoult and Kelvin terms corresponding to a macroscopic (bulk) solution of the same overall composition, denoted "σ,b", and (3) completely disregarding surfactant properties of the organic by ignoring its surface partitioning and using the constant surface tension of pure water (σ_w) throughout droplet activation, denoted "σ_w". In the following, the partitioning representation and the concentration-dependent surface tension parameterizations are described in more detail.

4.1 The droplet partitioning representation (σ,p)

The partitioning model (σ,p) is based on solving the Gibbs adsorption equation (Gibbs et al., 1928) for the bulk phase concentrations of all droplet components:

$$\sum n_i^T RT\, d\ln(a_i^B) + A\, d\sigma = 0 \tag{2}$$

where A [m^2] is the spherical droplet surface area, and n_i^T [mol] is the total molar amount and a_i^B is the bulk phase activity of droplet component i. Droplet solutions comprise water (w), surfactant anion (SFT$^-$), and sodium (Na$^+$) and chloride (Cl$^-$) ions. Bulk phase activities are approximated by the corresponding concentrations (c_i^B), as mentioned. For each droplet component, the total amount is equal to the sum of the individual amounts in the separate bulk and surface phases, $n_i^T = n_i^B + n_i^S$, and equivalently for the droplet component volumes.

When calculating the surfactant surface partitioning, electro-neutrality is assumed for both the droplet bulk and surface phases, such that equal amounts of sodium cations and surfactant anions partition to the surface. In our model description, the surface phase therefore comprises both the topmost molecular layer, dominated by the surfactant anions, and additional sub-surface layers, where sodium cation concentrations are enhanced compared to the bulk phase. Overall, the net charge of these layers constituting the surface phase is zero. It is however desirable that both droplet bulk-volume (V) and surface-area (A) are independent of the bulk-surface partitioning of droplet components, so the surface-volume is set to zero. In practice, this just means that when some species has enhanced surface-volume, an equal volume of another species is depleted from the surface phase.

One further approximation is that we assume the water and NaCl bulk phase ratio to be equal to the ratio of their total amounts, $n_w^T/n_{\mathrm{NaCl}}^T = n_w^B/n_{\mathrm{NaCl}}^B$. This simplifies our calculations, since the set of equations given by Eq. (2) now only depends on a single independent variable, the surfactant anion bulk phase activity $a_{\mathrm{SFT}^-}^B$.

4.2 Surface tension parameterizations

Model representations σ,p and σ,b employ concentration-dependent equilibrium surface tensions for the growing droplets (Prisle et al., 2008). Experimental ternary SFT-NaCl aqueous solution surface tensions were obtained from Prisle et al. (2009) for the fatty acid salts (FAS), and from Rehfeld (1967) and Matijevic and Pethica (1958) for SDS. Surface tensions were parameterized as fuctions of both surfactant and NaCl bulk phase concentrations by fitting these data with the Szyskowski equation (Szyskowski, 1908). Experimental surface tensions decrease with increasing respective bulk phase concentrations of both surfactant and NaCl over the reported ranges. For a given NaCl concentration, the surfactant strength in the ternary aqueous solutions, in terms of the surface tension reduction from the pure water value ($\sigma_w - \sigma$) attained for a given surfactant concentration, increases in the same order as for the corresponding binary aqueous solutions, as $\mathrm{C8} < \mathrm{C10} < \mathrm{C12} < \mathrm{SDS}$.

For the FAS-NaCl aqueous solutions, the Szyskowski equation was fitted to experimental surface tensions in the form:

$$\sigma = \sigma_w + \left(\frac{d\sigma_{\mathrm{NaCl}}}{dm_{\mathrm{NaCl}}}\right) m_{\mathrm{NaCl}} - a\ln(1 + m_{\mathrm{FAS}}/b) \tag{3}$$

where m_{NaCl} and m_{FAS} are the NaCl and FAS bulk phase molal concentrations (moles of solute species per kilogram of water) and $\sigma_w = 72.2$ mNm^{-1} is the pure water surface tension at 296.65 K. The surface tension gradient for aqueous NaCl, $\left(\frac{d\sigma_{\mathrm{NaCl}}}{dm_{\mathrm{NaCl}}}\right) = 1.61$ [mN m^{-1}/mol kg^{-1}], is obtained by linear fitting to data from Vanhanen et al. (2008). Szyskowski equation fitting parameters a and b depend on the FAS bulk phase solute mass fraction (w_{FAS}) relative to NaCl (where $w_{\mathrm{FAS}} + w_{\mathrm{NaCl}} = 1$):

$$a = a_1 + a_2 w_{\mathrm{FAS}} + a_3 w_{\mathrm{FAS}}^2 \tag{4}$$

$$b = b_1 + b_2 w_{\mathrm{FAS}} + b_3 w_{\mathrm{FAS}}^2 \tag{5}$$

Fitted parameters are given in Table 3. Note that, due to surfactant surface partitioning, relative surfactant and NaCl solute bulk phase mass-fractions are generally not equal to the corresponding total mass-fractions of surfactant and NaCl (w_{SFT} and w_{NaCl}) in the dry particles.

The SDS-NaCl aqueous solution surface tension parametrization is obtained from the Szyskowski equation with SDS and NaCl bulk phase molar concentrations (moles of solute species per liter of solution) c_{SDS} and c_{NaCl}:

$$\sigma = \sigma_w + \left(\frac{d\sigma_{\mathrm{NaCl}}}{dc_{\mathrm{NaCl}}}\right) c_{\mathrm{NaCl}} - a\ln(1 + c_{\mathrm{SDS}}/b) \tag{6}$$

Because solutions are dilute, molarities and molalities are approximately equal. Therefore, the same numerical value of the surface tension slope, $\left(\frac{d\sigma_{\mathrm{NaCl}}}{dc_{\mathrm{NaCl}}}\right) = 1.61$ [mN m^{-1}/mol L^{-1}], is also used here. Fitted parameters are $a = 13.9$ mN m^{-1} and $b = (9.27\mathrm{E}-6\ \mathrm{mol}^2\ \mathrm{L}^{-2})/(c_{\mathrm{NaCl}} + 9.73\mathrm{E}-3\ \mathrm{mol\ L}^{-1})$. A ternary SDS-NaCl aqueous solution surface tension parametrization based on the same data from Rehfeld

(1967) and Matijevic and Pethica (1958) is also provided by Li et al. (1998). This parametrization is however not continuous, which would cause problems in our calculations, and therefore the new continuous parametrization in Eq. (6) was made.

Surfactants can form micelles in concentrated aqueous solutions above the so-called critical micelle concentration (cmc). Micelles are aggregate structures in which the amphiphilic surfactant molecules orient themselves with the polar head-groups facing the aqueous medium, thus shielding a core consisting of the non-polar hydrocarbon tails (Corrin and Harkins, 1947). Surface tension parameterizations were obtained by fitting data corresponding to surface tension values above those at the respective ternary solution cmcs, estimated by visual inspection of the data. In all calculations, the surface tension at surfactant concentrations above the cmc is set constant to the value at the cmc.

5 Results and discussion

5.1 Experimental results

Figure 1a–d show measured critical supersaturations (SS_c^{exp}) as a function of the selected mobility diameter (D_p) for the mixed SFT-NaCl particles. Individual panels display results for different surfactant mass-fractions (w_{SFT}) in the dry particles.

5.1.1 Particle component molecular properties

In panels (a) and (b), it is seen that with surfactant mass-fractions $w_{\mathrm{SFT}} \leq 50\%$, differences in SS_c^{exp} for particles of a given dry size comprising the different surfactants are comparable to experimental uncertainties. Any differences in activation behavior due to individual molecular properties of the organic surfactants are thus dominated by the presence of the inorganic salt. Panels (c) and (d), on the other hand, show that when $w_{\mathrm{SFT}} \geq 80\%$, particles activate as a function of D_p with SS_c^{exp} increasing in the order of increasing surfactant molecular mass (M_{SFT}), as C8 < C10 < C12 < SDS.

We have previously observed single-component particles of these same surfactants to activate with SS_c^{exp} increasing in the order of increasing surfactant molecular mass (Sorjamaa et al., 2004; Prisle et al., 2008). The surfactant strength also increases with increasing M_{SFT} in both binary SFT and ternary SFT-NaCl aqueous solutions (see Sect. 4.2). For the solution droplets formed on pure surfactant particles of a given dry size, any enhanced surface tension reduction with increasing surfactant strength was insufficient to overcome the decrease in Raoult effect arising directly from the increase in M_{SFT} and possibly also from enhanced bulk depletion by surface partitioning of the stronger surfactants.

Inorganic salts influence organic surfactant properties, as seen from the ternary SFT-NaCl aqueous solution surface tensions in Sect. 4.2. Increased organic activity in a high-ionic strength aqueous salt solution will drive surfactant molecules out of solution by precipitation and/or enhanced surface partitioning. This is often called the "salting-out effect" (Lin et al., 2005; Tuckermann, 2007; Vanhanen et al., 2008). The large surfaces of microscopic droplets are expected to favor surface partitioning for considerations of cloud droplet activation. Enhanced surface partitioning may increase surfactant strength but will also increase bulk phase depletion of dissolved surfactant molecules. In addition, inorganic salts also directly influence cloud droplet activation. The molecular mass of NaCl is much lower than those of the surfactants (see Table 2). Therefore, NaCl by dry particle mass fraction contributes a much larger Raoult effect in the solution droplets formed, than the organics.

When NaCl comprises half, or more, of the dry particle mass, the large Raoult effect of the inorganic salt appears to dominate any differences in molecular properties of the individual organic surfactants in determining droplet activation. On the other hand, for mixed particles with the surfactant comprising more than half of the mass, the effects of individual surfactant molecular properties become evident. Still, just as for the pure surfactant particles, the increasing droplet surface tension reduction with increasing surfactant strength at a given w_{SFT} evidently cannot overcome the decrease in Raoult effect from increased M_{SFT} and enhanced surface partitioning.

5.1.2 Surfactant mass fraction

Comparing panels (a)–(d) in Fig. 1 shows that, in case of each individual surfactant, SS_c^{exp} for a given dry particle size increases with increasing surfactant mass-fraction (w_{SFT}) in the particles. Thus, as NaCl is replaced by surfactant, any reduction in droplet surface tension and Kelvin effect is dominated by the decrease in Raoult effect from increasing molecular mass ($M_{\mathrm{SFT}} > M_{\mathrm{NaCl}}$) and enhanced surface partitioning of the surfactant.

5.2 Comparison with Köhler model predictions

In Fig. 2, experimental critical supersaturations (SS_c^{exp}) for particles with 81% sodium dodecanoate (C12) are compared to predictions from Köhler theory with the three different surfactant representations ($SS_c^{\sigma,p}$, $SS_c^{\sigma,b}$, and $SS_c^{\sigma_w}$). The bulk representation (σ,b) greatly underpredicts experimental values for all dry particle sizes (D_p). Experimental values are also somewhat underpredicted by the representation ignoring surfactant properties altogether (σ_w). The partitioning representation (σ,p) on the other hand describes experimental activation behavior well.

5.2.1 General comparison

Experimental (SS_c^{exp}) and modeled (SS_c) critical supersaturations are compared in terms of the relative differences $(SS_c^{\mathrm{exp}} - SS_c)/SS_c^{\mathrm{exp}}$ [%/%] for all dry particle sizes and compositions in Fig. 3 a–d. Each panel shows the comparison for particles comprising one of the surfactants. Being compared to three different model predictions, the same experimental data point thus appears in Fig. 3 as three different points (in blue for σ,p, green for σ,b, and pink for σ_w, respctively). Error bars depict the experimental uncertainties scaled accordingly ($\pm 2\tau/SS_c^{\mathrm{exp}}$). It is immediately clear, that representation σ,b significantly underpredicts SS_c^{exp} for all dry particle sizes and compositions studied here. The modeled critical supersaturations, $SS_c^{\sigma,b}$, are well outside the range of experimental uncertainty in all cases. Model representation σ_w generally also underpredicts experimental critical supersaturations, but to a lesser degree.

The partitioning representation (σ,p) overall predicts SS_c^{exp} well. Specifically, for the mixed particles comprising SDS, σ,p is superior to the bulk property representations (σ,b and σ_w) over the ranges of particle sizes and compositions studied. In case of the particles comprising one of the fatty acid salts (FAS), the σ,p representation tends to somewhat overpredict experimental critical supersaturations. Detailed analysis (not shown here) indicate that this generally occurs for the smaller particles comprising the larger mass-fractions of the stronger surfactants. For the largest particles comprising FAS, all surfactant representations underpredict SS_c^{exp}. The dependency of the critical supersaturations on D_p in the log-log plots (as in Fig. 2) is generally steeper for model predictions than observed experimentally. There appears to be some size-dependent effect on activation not accounted for with the equilibrium Köhler model.

5.2.2 Effect of surfactant mass fraction

Figure 4 shows measured (SS_c^{exp}) and modeled (SS_c) critical supersaturations for particles of selected dry sizes comprising sodium dodecanoate (C12) in increasing mass fractions (w_{C12}). Upper curves and data points are results for $D_p = 40$ nm, representative of the “smaller” particle sizes, and lower curves and data points are results for $D_p = 100$ nm, representative of the “larger” particles studied. The bulk representation (σ,b) increasingly underpredicts experimental critical supersaturations with increasing surfactant mass-fraction in the dry particles. The partitioning representation (σ,p) generally describes experimental activation well, but overpredicts SS_c^{exp} for the smaller particles ($D_p = 40$ nm) with the largest w_{C12} (95%). This overprediction is likely due to uncertainties in the surface tension parameterization applied (see Sect. 5.5 below). The simple σ_w representation also describes experimental values well for the smaller w_{C12}, but underpredicts SS_c^{exp} when particles contain significant C12 mass fractions (e.g. $>50\%$).

In Fig. 5, the same results for the relative differences $(SS_c^{\text{exp}} - SS_c)/SS_c^{\text{exp}}$ shown in

Fig. 3 are displayed as a function of dry particle surfactant mass fraction (w_{SFT}), for the selected dry particle sizes of $D_p = 40$ and 100 nm. The conclusions for all the surfactants studied are identical to those seen in Fig. 4 for C12. When particles comprise less than about 50% by mass of surfactant, representations σ, p and σ_w predict very similar critical supersaturations and both describe experimental values well. For these particles, the simple σ_w representation, which ignores surfactant properties altogether, thus appears to be a good first-order approximation for representing cloud droplet activation behavior of the surfactants.

5.3 Individual Kelvin and Raoult contributions

5.3.1 Single particle predictions

The model predicted critical supersaturations, given by the calculated Köhler curve maxima, are governed by the combination of two opposing effects, the suppression of water partial pressure over an aqueous solution by dissolved compounds (the Raoult effect) and the enhanced vapor pressure over a curved surface (the Kelvin effect). Fig. 6 shows Köhler model predictions of droplet growth and activation, calculated with the different surfactant representations, for particles comprising surfactant C12 with $w_{\mathrm{C12}} = 81\%$ and $D_p = 40$ nm. The individual Kelvin (K) and Raoult (R) terms are seen in the left-hand panel (a) and the resulting Köhler curves in the right-hand panel (b). The measured critical supersaturation value (SS_c^{exp}) for these particles is depicted in panel (b) as a red line, with the 95%-confidence interval.

As seen from Eq. (1), the Kelvin term depends explicitly on droplet surface tension (σ). The pink Kelvin curve in Fig. 6a is calculated assuming the constant surface tension of pure water (σ_w) for the growing droplet at all diameters (d). This curve thus describes the change in vapor pressure enhancement arising purely from the droplet surface curvature changing with size. The green curve shows the predicted Kelvin effect with a concentration-dependent droplet surface tension (σ), corresponding to a macroscopic solution of the same overall composition as the droplet (σ, b). The effect of reduced σ at a given droplet diameter is to shift the Kelvin term vertically down to lower equilibrium supersaturations (SS). As the droplet grows, it becomes increasingly dilute and σ increases along with the droplet curvature radius. This flattens the size-dependency of the Kelvin term. The kink in the green Kelvin curve (for droplet diameters just below 300 nm) stems from the functional form of the surface tension parameterization and represents the point where the droplet surface tension becomes constant as the bulk phase surfactant concentration increases above the ternary solution cmc.

When surfactant partitioning to the droplet surface is accounted for (σ,p), the droplet solution properties at a given size (and thus overall composition) change significantly, compared to those of a macroscopic solution. This is clearly seen for the blue Kelvin curve in Fig. 6a, which is shifted to considerably higher equilibrium supersaturations (SS), compared to the green σ,b-Kelvin curve. The reason is evident from the corresponding Raoult terms: the green Raoult curve is predicted without consideration of surfactant partitioning in the droplet (and is thus the same for both σ,b and σ_w representations). The blue Raoult curve takes surfactant partitioning to the droplet surface into account (σ,p). For the smaller droplet sizes (e.g. $d < 300$ nm), surfactant concentrations in the droplet bulk are significantly depleted due to surface partitioning and the reduced Raoult effect significantly increases the droplet water activity (a_w). The effect of surfactant surface partitioning is thus seen as a horizontal shift of the Raoult term towards smaller droplet diameters, as larger a_ws are reached at earlier stages of droplet growth. Surfactant depletion from the droplet bulk also results in a greatly diminished surface tension reduction, as seen from the upward shift of the σ,p-Kelvin curve compared to the σ,b-Kelvin curve. Clearly, depletion of surfactant from the droplet bulk diminishes both the surface tension and water activity reduction attained at a given droplet diameter.

Figure 6b shows the Köhler curves resulting from combining the respective Kelvin and Raoult terms displayed in panel (a). For the same droplet sizes (d), the (green) Köhler curve predicted with the σ,b representation is shifted down to significantly lower equilibrium supersaturations, compared to the (pink) σ_w-Köhler curve, due to reduced droplet surface tension. However, when surfactant partitioning to the droplet surface is included, the combined effects on the respective Kelvin and Raoult terms result in a (blue) σ,p-Köhler curve that is shifted to even higher SS than predicted for σ_w by completely disregarding any surfactant properties. The droplet surface tension *is* reduced within the partitioning model, as seen by the Kelvin terms in panel (a), where $K^{\sigma,p} < K^{\sigma_w}$, but with the surfactant bulk-concentrations depleted due to surface partitioning, the effect is insufficient to counteract the simultaneous increase in water activity.

5.3.2 Predicted activation parameters

The respective Köhler curve maxima in Fig. 6b yield the critical supersaturations (SS_c) predicted with each surfactant representation. These maxima increase in the order $SS_c^{\sigma,b} \ll SS_c^{\sigma_w} < SS_c^{\sigma,p}$. This trend is seen for all dry particle sizes and compositions studied (see also Figs. 2 and 7b). In our previous study, surfactant representations σ,p and σ_w gave nearly identical predictions of critical supersaturations for single-component fatty acid salt particles (Prisle et al., 2008). This was a coincidence of the mutual differences in predicted Kelvin and Raoult terms cancelling at the respective points of droplet activation, for the specific particle compositions studied. The studies of Sorjamaa et al. (2004); Sorjamaa and Laaksonen (2006) did not observe this coincidence in their predictions, for either single-component SDS particles or for a range of surface tension parameters corresponding to three classes of atmospheric surfactants, respectively. This is consistent with the findings of Ruehl et al. (2009) in a study of high-relative humidity hygroscopic growth of particles with SDS. Here, we see that representations σ,p and σ_w indeed also produce different results for mixed SFT-NaCl particles with more than about 50% by mass of surfactant (Figs. 4 and 5).

The predicted critical supersaturations in Fig. 6b occur for different corresponding critical droplet diameters (d_c). Care must therefore be taken when comparing droplet parameters at activation predicted with the different surfactant representations. In Fig. 7, we compare model representations σ,p and σ_w for 81% C12 particles by the relative equilibrium saturation ratios (S) and individual Kelvin (K) and Raoult (R) terms. The left-hand panel (a) shows $S^{\sigma,p}(d)/S^{\sigma_w}(d)$, $K^{\sigma,p}(d)/K^{\sigma_w}(d)$, and $R^{\sigma,p}(d)/R^{\sigma_w}(d)$, as functions of droplet diameter (d) for 40 nm dry particles. In the right-hand panel (b), quantities predicted at the respective d_cs are compared by $S_c^{\sigma,p}(d_c^{\sigma,p})/S_c^{\sigma_w}(d_c^{\sigma_w})$, $K_c^{\sigma,p}(d_c^{\sigma,p})/K_c^{\sigma_w}(d_c^{\sigma_w})$, and $R_c^{\sigma,p}(d_c^{\sigma,p})/R_c^{\sigma_w}(d_c^{\sigma_w})$, displayed as functions of dry particle size (D_p). Since the predicted critical droplet diameters differ in the two representations, the ratio $d_c^{\sigma,p}/d_c^{\sigma_w}$ is also shown as a function of D_p (to be read off the right-hand y-axis) in panel (b).

Figure 7a emphasizes the results of Fig. 6 and for σ,p and σ_w. At a given droplet size (d), the magnitude of the relative increase in the Raoult term (water activity, a_w) from surfactant bulk-depletion due to surface partitioning is greater than that of the relative decrease in the Kelvin term from surface tension (σ) reduction, $|1-R^{\sigma,p}(d)/R^{\sigma_w}(d)| > |1-K^{\sigma,p}(d)/K^{\sigma_w}(d)|$. As a consequence, the equilibrium saturation ratio predicted for the droplet is always greater with the σ,p representation than with σ_w, such that $S^{\sigma,p}(d)/S^{\sigma_w}(d) > 1$.

Figure 7b compares droplet parameters for representations σ,p and σ_w predicted at the respective points of activation ($d_c^{\sigma,p}$ and $d_c^{\sigma_w}$). Critical saturation ratios are always larger for σ,p than for σ_w, as $S_c^{\sigma,p}(d_c^{\sigma,p})/S_c^{\sigma_w}(d_c^{\sigma_w}) > 1$. This is a result of the Kelvin and Raoult terms predicted at activation *both* being larger in the partitioning representation, as seen from $K_c^{\sigma,p}(d_c^{\sigma,p})/K_c^{\sigma_w}(d_c^{\sigma_w}) > 1$ and $R_c^{\sigma,p}(d_c^{\sigma,p})/R_c^{\sigma_w}(d_c^{\sigma_w}) > 1$. At first, it may seem surprising that the Kelvin terms are greater in $k\sigma,p$ than in σ_w, where surface tension is not reduced. Again, it must be stressed that the activating droplets being compared are of different sizes. Specifically, $d_c^{\sigma,p}/d_c^{\sigma_w} < 1$ over the full range of dry particle sizes (D_p). Therefore, $K_c^{\sigma,p}(d_c^{\sigma,p}) > K_c^{\sigma_w}(d_c^{\sigma_w})$ does *not* imply that surface tension is not reduced in the activating droplets in σ,p. Rather, droplets with the smaller critical diameters ($d_c^{\sigma,p} < d_c^{\sigma_w}$) have more curved surfaces and are subject to a greater curvature enhancement of vapor pressure, despite the reduced surface tension. The critical droplet diameters predicted with σ,p and σ_w for 40 nm dry particles are marked in panel (a) of Fig. 7. Surface tension is clearly reduced in σ,p at $d_c^{\sigma,p}$, where $K^{\sigma,p}(d_c^{\sigma,p})/K^{\sigma_w}(d_c^{\sigma,p}) < 1$.

Even if droplets are predicted to activate for smaller critical sizes, the Raoult terms at activation are still larger in the σ,p representation than in σ_w, as noted. The smaller activating droplets ($d_c^{\sigma,p} < d_c^{\sigma_w}$) formed on particles of a given dry size (D_p) and composition have larger total surfactant concentrations ($c^T(d_c^{\sigma,p}) > c^T(d_c^{\sigma_w})$). However, the smaller droplets also have larger surface-area-to-bulk-volume ratios (A/V) and the surfactant bulk concentrations are thus relatively more depleted due to surface partitioning ($c^B/c^T(d_c^{\sigma,p}) < c^B/c^T(d_c^{\sigma_w})$). Figure 7b shows that, despite the larger total surfactant concentrations, surface partitioning in the smaller activating droplets even results in smaller bulk concentrations in absolute terms ($c^B(d_c^{\sigma,p}) < c^B(d_c^{\sigma_w})$) – and thus in the larger droplet water activities for activating droplets predicted with σ,p compared to σ_w.

For mixed SFT-NaCl particles of a given dry size and composition, the predicted shapes of the Köhler curves and their maximum values and positions are seen to be governed by complex relations between the individual Kelvin and Raoult terms. Although droplet surface tension is reduced in σ,p, the effect is overwhelmed by surfactant depletion from the droplet bulk due to surface partitioning. This is the case both at a given droplet size (d) and overall composition, and when comparing activation parameters predicted at the respective points of droplet activation (d_c). Particularly, the comprehensive account of surfactant properties actually predicts higher critical supersaturations than the simple approach that ignores surfactant properties altogether ($S_c^{\sigma,p} > S_c^{\sigma_w}$). This is opposed to the decrease in critical supersaturations that could be immediately expected from the explicit dependency of the Kelvin term on reduced droplet surface tension (Shulman et al., 1996).

5.4 Activation properties of mixed surfactant-salt particles

Comparing experimental results and model predictions using different surfactant representations illustrate some of the dynamics behind the combined effect of surfactant properties on cloud droplet activation for the mixed particles. The partitioning representation is the most comprehensive of the three surfactant representations applied in our thermodynamic model. Predicted surface tensions of the droplets formed are indeed reduced, as anticipated from the presence of water-soluble surfactants in the particles studied. However, due to surfactant partitioning, the surface tension reductions attained are much smaller than for macroscopic solutions of the same overall composition as the droplets. As a result, the predicted diminished curvature enhancement of vapor pressure due to decreased surface tension is dominated by the simultaneously diminished Raoult suppression of water activity.

This explains how the bulk representation of surfactant properties greatly underpredicts experimental critical supersaturations (see Figs. 2, 3, 4, 5, and 6b). The bulk model overestimates the reductions in both Kelvin and Raoult terms from the surfactant by disregarding depletion of the surfactant bulk-concentration due to surface partitioning. The above also explains how the simple representation that completely ignores surfactant properties can also lead to significant *under*predictions of experimental critical supersaturations. This might have seemed surprising at first, since the actual droplet surface tension is not expected to increase significantly above the pure water value, even with the presence of the inorganic salt, which can slightly increase aqueous solution surface tension (Low, 1969). By using the constant surface tension of pure water for activating droplets, the simple model misses the reduction in Kelvin effect from reduced droplet surface tension, but this is overshadowed by simultaneously overestimating the Raoult effect from disregarding surfactant partitioning. When $SS_c^{\text{exp}} > SS_c^{\sigma_w}$, it is thus a clear experimental indication of the effect of surfactant partitioning in activating cloud droplets, where surface activity causes the Raoult effect suppression to be greater than the Kelvin effect suppression.

Other studies have considered surfactant properties by using reduced surface tensions for activating droplets corresponding to macroscopic (bulk) aqueous solutions with the same overall composition (Shulman et al., 1996; Facchini et al., 1999; Dinar et al., 2006; Svenningsson et al., 2006). Calculations have also been simplified by assuming droplets sufficiently dilute that the constant surface tension of pure water could be applied (Bilde and Svenningsson, 2004; Hartz et al., 2005). Li et al. (1998) and Rood and Williams (2001) partially accounted for surface partitioning in cloud droplet formation of mixed SDS-NaCl particles by including the effect on droplet surface tension. Rood and Williams (2001) present experimental data for the CCN activity of mixed SDS-NaCl particles with similar compositions as was studied in this work. Their measured critical supersaturations follow the same trends with particle size and surfactant mass fraction as the results presented here for particles comprising SDS. The values of Rood and Williams (2001) are consistently lower than ours, but as no experimental uncertainties are given in their study, we cannot say if the difference is significant. The results of the present study show that surfactant properties are overall well represented in Köhler predictions of cloud droplet activation with a full account for the effects of surfactant partitioning on both Kelvin and Raoult terms.

Generally, the combined effects of reduced surface tension and surfactant surface partitioning on droplet ativation will depend on dry particle size (D_p), surfactant mass fraction (w_{SFT}), and surfactant strength (as for example expressed by Szyskowski parameters a and b). However, the overall effect of surfactant properties in general, and of surface partitioning in particular, results from intricate mutual dependencies of the Kelvin and Raoult effects on these fundamental particle and component properties. The largest effect of surface activity would be expected for the smallest particles containing the largest mass fractions of the strongest surfactants. Droplets formed on smaller dry particles activate at critical diameters corresponding to smaller diameter growth factors (d_c/D_p), for which droplets are more concentrated ($c^T \propto (d_c/D_p)^{-3}$). These droplets however also have larger surface area-to-bulk volume ratios ($A/V \propto d_c^{-1}$) and the surfatant will be relatively more depleted from the bulk phase. It has in the present work not been possible to establish explicit gauges in parameters D_p, w_{SFT}, and a and b, for example, for conditions where the effects of surfactant properties become significant for predictions of cloud droplet activation. Some reasons are the experimental uncertainties on measured critical supersaturations, and model sensitivities to uncertainties in experimental parameters and in the surface tension parameterizations applied. For the fatty acid salts, the ternary solution surface tension parameterizations are not constrained by measurements for bulk phase mass-fractions (w_{FAS}) relative to NaCl below 20%. In small droplets, the surfactant bulk phase depletion due to surface partitioning can however yield very low w_{FAS}s. The FAS surface tension parameterizations may therefore not reproduce the correct surface tension behavior for such droplets. The limited span of surface tension parameters investigated here may also make it difficult to resolve any variation with surfactant strength. Establishment of gauges for the representation of surfactant properties in cloud droplet activation would nevertheless be of great use for atmospheric model calculations and is something we shall continue to explore.

As a simple preliminary gauge, disregarding surfactant partitioning and assuming the constant surface tension of pure water seems to be a good first-order approximation for representing surfactant properties in activation of mixed particles comprising less than 50% by mass of surfactant. The predicted effects of surfactant properties on the individual Kelvin and Raoult terms cancel in the comprehensive partitioning model and give the same overall results as the simple representation. The agreement of experimental results for particles with similar mass fractions of the different surfactants furthermore suggests that for dry particle surfactant mass fractions (w_{SFT}) less than 50%, the large Raoult effect of the inorganic salt dominates any differences in activation behavior arising from differences in organic molecular properties (see Fig. 1).

The cloud droplet activation properties for the mixed particles naturally depend on the properties of both surfactant and NaCl. The inorganic salt affects surfactant properties of the organic by increasing surfactant strength in macroscopic ternary aqueous solutions. In addition, NaCl by mass-fraction contributes a large Raoult effect relative to the surfactant in macroscopic solutions. Both effects influence the relative importance of the Kelvin and Raoult effects for the activating droplets. In particular, the predicted effects of surfactant properties on the individual Kelvin and Raoult terms do not cancel for mixed particles with more than 50% by mass of the surfactants studied, as was observed for single-component particles of the same surfactants. In fact, even if NaCl increases surfactant strength in the macroscopic solutions, the effect of enhanced surface partitioning is even greater on increasing the water activity in the activating droplets.

5.5 Model sensitivities

The partitioning representation is expected to provide the most comprehensive description of surfactant properties. Nevertheless, calculations somewhat overpredict experimental critical supersaturations ($SS_c^{\sigma,p} > SS_c^{\mathrm{exp}}$) for particles comprising the fatty acid salts (FAS) in the highest mass-fractions studied ($\sim 95\%$). The most significant model sensitivities concerns experimental uncertainties in the dry particle surfactant mass-fractions (w_{SFT}) and mass densities (ρ_{SFT}), uncertainties in the surface tension parameterizations applied (as explained above in Sect. 5.4), and the model assumption of droplet solution ideality.

Uncertainties in experimental dry particle surfactant mass-fraction or in the surface tension parameterizations applied would be expected to become increasingly important for the larger surfactant mass-fractions in the particles, where surfactant properties play a relatively larger role, compared to the inorganic salt. In the model calculations, we assume the dry particle surfactant and NaCl mass-fractions to be equal to their relative solute mass-fractions in the atomizer solutions. This assumption has previously been argued as reasonable for other mixed organic-inorganic particle compositions (Bilde and Svenningsson, 2004; Henning et al., 2005). In addition, the studied fatty acid salts (FAS) showed no evaporation from pure-component particles in equivalent experiments (Prisle et al., 2008). During the particle generation process, precipitation of surfactant, due to decreased solubility in the high-ionic strength NaCl aqueous solution, or evaporation of the surfactant from the wet or dry aerosol, would act to decrease the actual surfactant mass-fractions in the dry particles. On the other hand, partitioning in the generated droplets during atomization could increase the relative amount of surfactant in the droplets, compared to the atomizer solution. Assuming too high w_{SFT} could explain the overpredictions of SS_c^{exp}. However, model calculations using the partitioning representation do not overpredict SS_c^{exp} for mixed particles comprising SDS, which is the better-characterized of the surfactants studied. This points to the modest overpredictions by the partitioning model for FAS being due to uncertainties in the surface tension parameterizations becoming evident for the highly bulk-depleted droplets formed on small particles with the largest w_{FAS}.

The assumption of unit mass-density for the organic surfactants is discussed by Prisle et al. (2008). The value of pure surfactant bulk-density, together with the assumption of volume additivity of individual components in the mixed particles, ultimately affects the relative molar amounts of surfactant and NaCl solute predicted in the activating droplets. Likely, the actual organic densities are not very different from 1 g cm^{-3}. Nevertheless, detailed sensitivity analysis indicate that uncertainty in organic and mixed particle mass-density is a principal cause of uncertainties in model predicted critical supersaturations. Pure surfactant bulk-densities and mixed particle densities are both issues we will address in future studies.

Ideality has been assumed for all components of the droplet solutions at all stages of droplet growth, due to lack of activity data for the droplet solutions in question. The droplet bulk is sufficiently dilute at the point of activation for this to be a reasonable approximation (Prisle et al., 2008). Non-ideality would be expected to increase droplet water activity above the corresponding water mole fraction ($a_w > x_w$). Assuming ideality for water would this way decrease predicted critical supersaturations compared to the experimental values. This is opposite of what is observed here for FAS with σ, p. On the other hand, the effect is by no means capable of resolving the large underpredictions of SS_c^{exp} by σ, b.

5.5.1 Micelle Formation in Droplets

As described in Sect. 4.2 above, surfactants can form micelles when bulk-concentrations exceed the critical micelle concentration (cmc). In all calculations, droplet bulk phase concentrations of both surfactant and NaCl are assumed to be continuous functions over the entire range of growing droplet sizes. If the surfactant bulk phase concentration was limited to the ternary solution cmc, a sufficiently small cmc value could inhibit droplet activation and increase predicted critical supersaturations by a mechanism analogous to water solubility limiting the droplet bulk phase concentration of a slightly soluble particle component (Bilde and Svenningsson, 2004).

Tabazadeh (2005) suggested that formation of micelle-like structures in droplet solutions of humic-like substances (HULIS) would limit the maximum droplet surface tension reduction attainable to about 10 mN m^{-1}. These considerations imply that micelle formation is favored over surface partitioning of the surfactant in droplets where the total surfactant concentration exceeds the cmc. The mechanism proposed by Tabazadeh (2005) may however not be relevant for the present solutions of amphiphilic anionic surfactants mixed with an inorganic salt of common counter-cation. Surface tension reductions much greater than 10 mN m^{-1} below the value for pure water was readily observed during measurement on macroscopic ternary FAS-NaCl aqueous solutions (Prisle et al., 2009).

Test calculations were made for selected particle sizes and compositions where droplet bulk-concentrations of surfactant were limited to the respective cmcs ($c^B_{\text{SFT}} \leq$ cmc). With the partitioning representation, micelle formation has no effect on predicted critical supersaturations ($SS_c^{\sigma,p}$), as cmc is not exceeded at droplet activation. Limiting surfactant bulk-concentrations affects the shape of the Köhler curves predicted with the bulk representation, but has no effect on the value of the critical supersaturations ($SS_c^{\sigma,b}$). With the simple pure water representation, however, limiting c^B_{SFT} to cmc acts to increase $SS_c^{\sigma_w}$ to values above those predicted with σ,p for the same particles. Therefore, σ_w with limited c^B_{SFT} overpredicts experimental critical supersaturations (SS_c^{exp}) even more than does σ,p. Of course, in the simple σ_w representation, droplet surface tension (σ) is not reduced. Reducing σ could potentially resolve the difference between SS_c^{exp} and $SS_c^{\sigma_w}$ predicted for $c^B_{\mathrm{SFT}} \leq$ cmc. Physically, the surfactant molecules would then have to be adsorbed at the droplet surface, as described within the σ,p representation. We therefore believe that the partitioning representation provides the most comprehensive account of surfactant properties and that micelle formation is not an issue for the experiments in this study.

6 Conclusions

We have measured critical supersaturations for laboratory-generated particles comprising the organic surfactants sodium octanoate, sodium decanoate, sodium dodecanoate, and sodium dodecyl sulfate, mixed with sodium chloride. Results were modeled from Köhler theory with three different representations of surfactant properties in terms of droplet surface tension reduction and surfactant surface partitioning. The predicted overall effect of surfactant properties for cloud droplet activation of the mixed particles results from complex mutual dependencies of the effects on the individual Kelvin and Raoult terms of the particle Köhler curves. The comprehensive thermodynamic account of surfactant properties including the effects of surface partitioning in activating droplets generally describes experimental observations well. Using reduced droplet surface tension while ignoring the effects of surfactant surface partitioning in all cases greatly underpredicts experimental critical supersaturations. In addition, ignoring surfactant partitioning and simply assuming the constant surface tension of pure water can also lead to significant underpredictions of experimental values. However, for mixed particles comprising less than about 50% by mass of surfactant, this simple approach appears to be a good first-order approximation for representing surfactant properties in activating droplets. This entails a significant simplification for model calculations of cloud droplet formation and properties.

Appendix A

Simple partitioning example

The effect of surfactant partitioning on the magnitude of both water activity and surface tension, resulting from a given overall solution composition, can be illustrated with the following simple example. We assume that spherical droplets of different diameters (d [μm]) are created from the same binary surfactant aqueous solution with a fixed total surfactant molarity (c^T [mmol L^{-1}]). The total amount of surfactant in the droplet (n^T [mol]) can be calculated from c^T and the droplet volume (V [L]). We imagine the surface as an infinitely thin spherical shell with area A [m^2]. The number area concentration of surfactant molecules in the surface phase is called the surfactant surface excess (Γ [m^{-2}]). If we simply assume a fixed surface excess for droplets of all sizes, the amount of surfactant in the surface (n^S [mol]) is calculated by scaling Γ to the spherical droplet surface area, as $n^S = \Gamma A$. Then the size-dependent surfactant bulk phase concentration (c^B [mmol L^{-1}]) is $c^B(d) = c^T - 6 \cdot 10^9 \Gamma / N_a d$, where N_a is Avogadro's number.

Representative values for surfactant surface excess and total molarity are taken from our previous study on single-component fatty acid salt particles (Prisle et al., 2008), specifically as the values at the point of activation for 100 nm sodium decanoate (C10) particles, $\Gamma = 10^{18}$ m^{-2} and $c^T = 40$ mmol L^{-1}. Droplet surface tension is calculated from the surfactant bulk phase concentration using the concentration dependent parametrization $\sigma = \sigma(c^B)$ for binary sodium decanoate aqueous solutions given in Prisle et al. (2008). We ignore non-ideal interactions in the droplet solutions, such that droplet water activity (a_w) is given by the equivalent water mole fraction (x_w). Then the ratio c^B/c^T provides a measure of how much surfactant surface partitioning at a given droplet size (d) diminishes the solute suppression and surface tension reduction that can be achieved for the same total surfactant concentration.

Results of these simple calculations are presented in Table A1 and in Fig. A1. Surfactant surface partitioning in this case becomes important for sub-micron droplets ($d < 1\ \mu$m). When the surfactant bulk-concentration decreases due to surface partitioning, both water activity and surface tension in the droplet are increased accordingly. Similar considerations have been presented by Bianco and Marmur (1992) and Laaksonen (1993).

Acknowledgements. The authors gratefully acknowledge the funding received for this work from EUCAARI (European Integrated project on Aerosol Cloud Climate and Air Quality interactions) No. 036833-2, the Danish Natural Science Research Council (Copenhagen Center for Atmospheric Research), and ACCENT Access to infrastructures. We thank Matthew S. Johnson for valuable comments.

References

Asa-Awuku, A., Sullivan, A. P., Hennigan, C. J., Weber, R. J., and Nenes, A.: Investigation of molar volume and surfactant characteristics of water-soluble organic compounds in biomass burning aerosol, Atmos. Chem. Phys., 8, 799–812, 2008, http://www.atmos-chem-phys.net/8/799/2008/. 24671

Bianco, H. and Marmur, A.: The Dependence of the Surface Tension of Surfactant Solutions on Drop Size, Journal of Colloid and Interface Science, 151, 517–522, 1992. 24700

Bilde, M. and Svenningsson, B.: CCN Activation of Slightly Soluble Organics: The Importance of Small Amounts of Inorganic Salt and Particle Phase, Tellus, 56B, 128–134, 2004. 24675, 24693, 24695, 24697

Cheng, Y., Li, S.-M., Leithead, A., Brickell, P. C., and Leaitch, W. R.: Characterizations of *cis*-pinonic acid and n-fatty acids on fine aerosols in the Lower Fraser Valley during Pacific 2001 Air Quality Study, Atmos. Environ., 38, 5789–5800, 2004. 24671

Corrin, M. L. and Harkins, W. D.: The Effect of Salts on the Critical Concentration for the Formation of Micelles in Colloidal Electrolytes, J. Amer. Chem. Soc., 69, 683–688, 1947. 24683

Dinar, E., Taraniuk, I., Graber, E. R., Katsman, S., Moise, T., Anttila, T., Mentel, T. F., and Rudich, Y.: Cloud Condensation Nuclei properties of model and atmospheric HULIS, Atmos.

Chem. Phys., 6, 2465–2482, 2006, http://www.atmos-chem-phys.net/6/2465/2006/. 24671, 24693

Facchini, M., Mircea, M., Fuzzi, S., and Charlson, R.: Cloud Albedo Enhancement by Surface-Active Organic Solutes in Growing Droplets, Nature, 401, 257–259, 1999. 24671, 24693

Facchini, M., Decesari, S., Mircea, M., Fuzzi, S., and Loglio, G.: Surface Tension of Atmospheric Wet Aerosol and Cloud/Fog Droplets in Relation to their Organic Carbon Content and Chemical Composition, Atmos. Environ., 34, 4853–4857, 2000. 24671

Gibbs, J., Bumstead, H., Longley, W., and Name, R. V.: The Collected Works of J. Willard Gibbs, Longmans, Green and Co., 1928. 24680

Hartz, K. E. H., Rosenørn, T., Ferchak, S. R., Raymond, T. M., Bilde, M., Donahue, N. M., and Pandis, S. N.: Cloud Condensation Nuclei Activation of Monoterpene and Sesquiterpene Secondary Organic Aerosol, J. Geophys. Res., 110, D14208, doi:10.1029/2004JD005754, 2005. 24693

Henning, S., Rosenørn, T., D'Anna, B., Gola, A. A., Svenningsson, B., and Bilde, M.: Cloud droplet activation and surface tension of mixtures of slightly soluble organics and inorganic salt, Atmos. Chem. Phys., 5, 575–582, 2005, http://www.atmos-chem-phys.net/5/575/2005/. 24695

IPCC: Climate Change 2007, The Physical Science Basis, Contribution of Working Group I to the Fourth Assessment Report of the Intergovernmental Panel on Climate Change, Cambridge University Press, 2007. 24671

Kiss, G., Tombácz, E., and Hansson, H.-C.: Surface Tension Effects of Humic-Like Substances in the Aqueous Extract of Tropospheric Fine Aerosol, J. Atmos. Chem., 50, 279–294, 2005. 24671

Köhler, H.: The Nucleus in and the Growth of Hygroscopic Droplets, Transactions of the Faraday Society, 32, 1152–1161, 1936. 24675

Laaksonen, A.: The Composition Size Dependence of Aerosols Created by Dispersion of Surfactant Solutions, J. Colloid Interf. Science, 159, 517–519, 1993. 24700

Li, Z., Williams, A., and Rood, M.: Influence of Soluble Surfactant Properties on the Activation of Aerosol Particles Containing Inorganic Solute, J. Atmos. Sci., 55, 1859–1866, 1998. 24672, 24683, 24693

Lin, B., McCormick, A. V., Davis, H. T., and Strey, R.: Solubility of sodium soaps in aqueous salt solutions, J. Colloid Interf. Science, 291, 543–549, 2005. 24684

Low, R.: A Theoretical Study of Nineteen Condensation Nuclei, Journal de Recherches Atmosphériques, 65–78, 1969. 24692

Matijevic, E. and Pethica, B. A.: The properties of ionized monolayers, Part 1. Sodium dodecyl sulphate at the air/water interface, Trans. Faraday Soc., 54, 1383–1389, 1958. 24681, 24683

Mochida, M., Kitamori, Y., Kawamura, K., Nojiri, Y., and Suzuki, K.: Fatty acids in the marine atmosphere: Factors governing their concentrations and evaluation of organic films on sea-salt particles, J. Geophys. Res., 107, D17S4325, doi:10.1029/2001JD001278, 2002. 24671

Mochida, M., Kawamura, K., Umemoto, N., Kobayashi, M., Matsunaga, S., Lim, H.-J., Turpin, B., Bates, T., and Simoneit, B.: Spatial distributions of oxygenated organic compounds (dicarboxylic acids, fatty acids, and levoglucosan) in marine aerosols over the western Pacific and off the coast of East Asia: Continental outflow of organic aerosols during the ACE-Asia campaign, J. Geophys. Res., 108, D23S8638, doi:10.1029/2002JD003249, 2003. 24671

Murphy, D. M., Cziczo, D. J., Froyd, K. D., Hudson, P. K., Matthew, B. M., Middlebrook, M., Peltier, R. E., Sullivan, A., Thomson, D. S., and Weber, R. J.: Single-particle mass spectrometry of tropospheric aerosol particles, J. Geophys. Res., 111, D23S32, doi:10.1029/2006JD007340, 2006. 24671

Oros, D. and Simoneit, B.: Identification and emission rates of molecular tracers in coal smoke particulate matter, Fuel, 79, 515–536, 2000. 24671

Prisle, N. L.: Cloud Condensation Nuclei Properties of Organic Aerosol Particles: Effects of Acid Dissociation and Surfactant Partitioning, M.Sc. Thesis, Department of Chemistry, University of Copenhagen, 2006. 24675

Prisle, N. L., Raatikainen, T., Sorjamaa, R., Svenningsson, B., Laaksonen, A., and Bilde, M.: Surfactant partitioning in cloud droplet activation: a study of C8, C10, C12 and C14 normal fatty acid sodium salts, Tellus, 60B, 416–431, doi:10.1111/j.1600-0889.2008.00352.x, 2008. 24671, 24672, 24673, 24674, 24675, 24678, 24679, 24681, 24684, 24689, 24695, 24696, 24699

Prisle, N. L., Vanhanen, J., Bilde, M., Laaksonen, A., and Hyvärinen, A.-P.: Surface tensions of ternary aqueous fatty acid sodium salt and NaCl solutions measured with the Wilhelmy plate and capillary rise methods, in preparation, 2009. 24681, 24697

Rehfeld, S. J.: Adsorption of Sodium Dodecyl Sulfate at Various Hydrocarbon-Water Interfaces, J. Phys. Chem., 71, 738–745, 1967. 24681, 24682

Rood, M. J. and Williams, A. L.: Reply, J. Atmos. Sci., 58, 1468–1473, 2001. 24672, 24693

Ruehl, C. R., Chuang, P. Y., and Nenes, A.: Aerosol hygroscopicity at high (99 to 100%) relative humidities, Atmos. Chem. Phys. Discuss., 9, 15595–15640, 2009, http://www.atmos-chem-phys-discuss.net/9/15595/2009/. 24672, 24689

Shulman, M., Jacobson, M., Charlson, R., Synovec, R., and Young, T.: Dissolution Behavior and Surface Tension Effects of Organic Compounds in Nucleating Cloud Droplets, Geophys. Res. Lett., 23, 277–280, 1996. 24691, 24693

Snider, J. R., Petters, M. D., Wechsler, P., and Liu, P. S. K.: Supersaturation in the Wyoming CCN Instrument, J. Atmos. Oceanic Technol., 23, 1323–1339, 2006. 24674

Sorjamaa, R. and Laaksonen, A.: The influence of surfactant properties on critical supersaturations of cloud condensation nuclei, J. Aerosol Sci., 37, 1730–1736, 2006. 24689

Sorjamaa, R., Svenningsson, B., Raatikainen, T., Henning, S., Bilde, M., and Laaksonen, A.: The role of surfactants in Köhler theory reconsidered, Atmos. Chem. Phys., 4, 2107–2117, 2004, http://www.atmos-chem-phys.net/4/2107/2004/. 24672, 24673, 24678, 24684, 24689

Svenningsson, B., Rissler, J., Swietlicki, E., Mircea, M., Bilde, M., Facchini, M. C., Decesari, S., Fuzzi, S., Zhou, J., Mønster, J., and Rosenørn, T.: Hygroscopic growth and critical supersaturations for mixed aerosol particles of inorganic and organic compounds of atmospheric relevance, Atmos. Chem. Phys., 6, 1937–1952, 2006, http://www.atmos-chem-phys.net/6/1937/2006/. 24693

Szyskowski, B. V.: Experimentelle studien über kapillare eigenschaften der wässerigen lösungen von fettsauren, Zeitschrift für Physikalische Chemie, 64, 385–414, 1908. 24681

Tabazadeh, A.: Organic aggregate formation in aerosols and its impact on the physicochemical properties of atmospheric particles, Atmos. Environ., 39, 5472–5480, 2005. 24697

Tuckermann, R.: Surface tension of aqueous solutions of water-soluble organic and inorganic compounds, Atmos. Environ., 41, 6265–6275, 2007. 24684

Vanhanen, J., Hyvärinen, A.-P., Anttila, T., Raatikainen, T., Viisanen, Y., and Lihavainen, H.: Ternary solution of sodium chloride, succinic acid and water; surface tension and its influence on cloud droplet activation, Atmos. Chem. Phys., 8, 4595–4604, 2008, http://www.atmos-chem-phys.net/8/4595/2008/. 24682, 24684

Yassaa, N., Meklati, B. Y., Cecinato, A., and Marino, F.: Particulate n-alkanes, n-alkanoic acids and polycyclic aromatic hydrocarbons in the atmosphere of Algiers City Area, Atmos. Environ., 35, 1843–1851, 2001. 24671

Table 1. Exact surfactant mass-fractions (w_{SFT} [%]) in the studied particles.

SFT	~ 20%	~ 50%	~ 80%	~ 95%
C8	20	51	79	95
C10	20	50	73	94
C12	23	53	81	95
SDS	20	51	81	–

Table 2. Physical properties of the studied compounds used in model calculations: molar mass M [g mol^{-1}], dissociation factor δ, and bulk mass density ρ [g cm^{-3}]. In all cases we have assumed $\delta = 2$, and for the fatty acid salts we assumed $\rho_{\mathrm{FAS}} = 1$ g cm^{-3}.

molecular formula	M [g mol^{-1}]	δ	ρ [g cm^{-3}]
$CH_3(CH_2)_6COONa$	166.2	2	1
$CH_3(CH_2)_8COONa$	194.2	2	1
$CH_3(CH_2)_{10}COONa$	222.3	2	1
$CH_3(CH_2)_{10}SO_4Na$	288.4	2	1.176
NaCl	58.44	2	2.165

Table 3. Szyskowski (Eq. 3) fitting parameters for FAS-NaCl aqueous surface tension parameterizations. Units of the a and b parameters are mN m^{-1} and mol kg^{-1}, respectively.

	a_1	a_2	a_3	b_1	b_2	b_3
C8	36.82	17.63	0	0.0119	0.0744	0
C10	40.10	8.06	−26.32	0.006	0.041	−0.034
C12	48.98	−0.88	0	0.004	0.004	0

Table A1. Simple partitioning calculations. Surfactant bulk molarities (c^B), ratio of surfactant bulk and total (c^T) molarities, and droplet surface tension, $\sigma = \sigma(c^B)$, for droplets of different sizes (d) created from the same $c^T = 40$ mmol L^{-1} sodium decanoate (C10) solution. The surfactant surface excess is fixed to $\Gamma = 10^{18}$ m^{-2} for all droplet sizes.

d [μm]	A/V [μm^{-1}]	c^B [mmol L^{-1}]	c^B/c^T	σ [mN m^{-1}]
0.3	20	6.8	0.170	68
0.5	12	20.1	0.502	61
1	6	30.0	0.751	57
10	0.6	39.0	0.975	54
50	0.12	39.8	0.995	54
∞	0	40.0	1.000	54

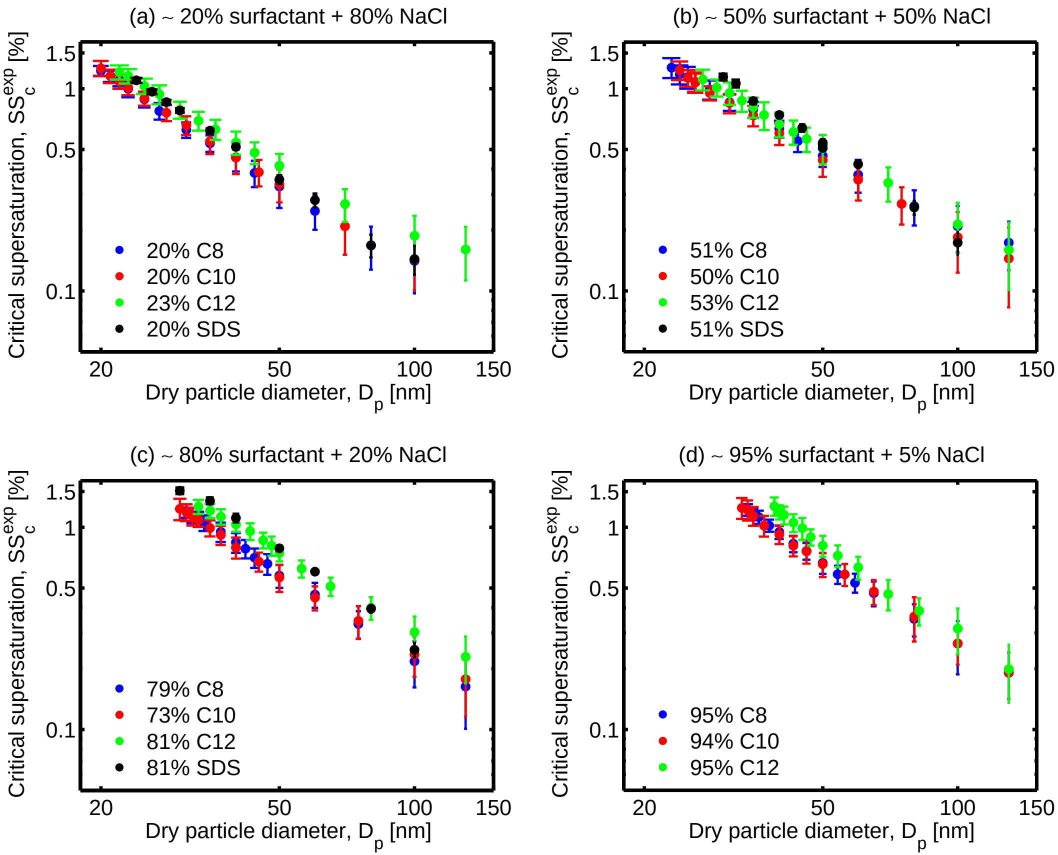

Fig. 1. Experimental critical supersaturations (SS_c^{exp} [%]) as a function of dry particle diameter (D_p [nm]) for all particle compositions. Individual panels show results for approximate dry particle surfactant mass fractions (w_{SFT}) of **(a)** 20%, **(b)** 50%, **(c)** 80% and **(d)** 95%.

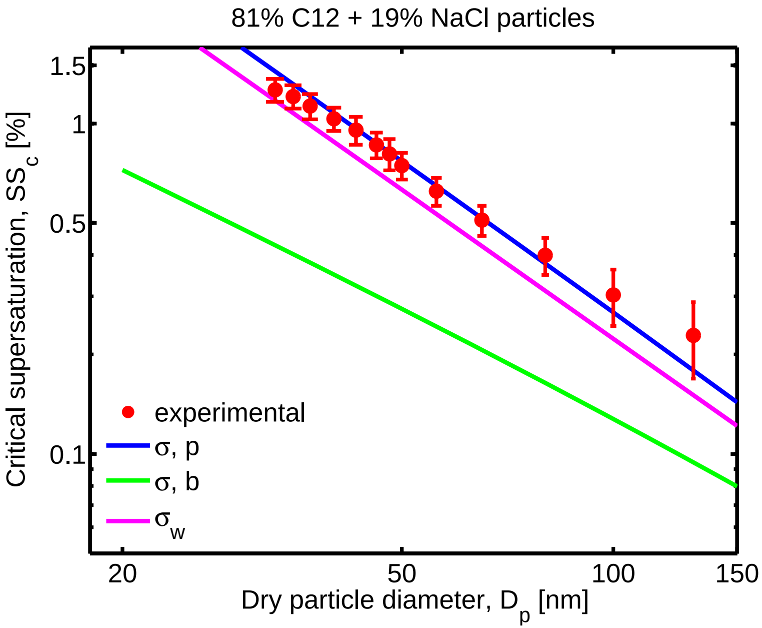

Fig. 2. Critical supersaturations (SS_c [%]) for particles with 81% sodium dodecanoate (C12), measured in experiments and modeled with the three different surfactant representations (σ, p, σ, b, and σ_w).

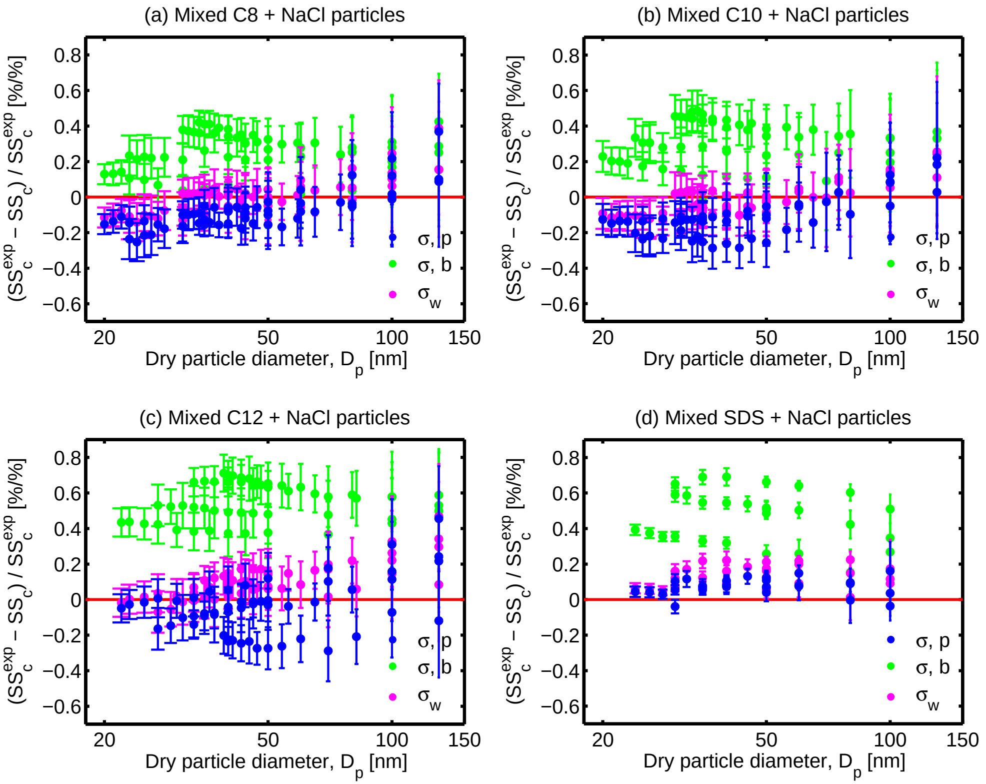

Fig. 3. Comparison of experimental (SS_c^{exp} [%]) and modeled (SS_c [%]) critical supersaturations with each of the three surfactant representations (σ,p, σ,b, and σ_w), for all dry particle diameters (D_p) and compositions studied. Individual panels show results for particles comprising each of the surfactants, **(a)** sodium octanoate (C8), **(b)** sodium decanoate (C10), **(c)** sodium dodecanoate (C12), and **(d)** sodium dodecyl sulfate (SDS).

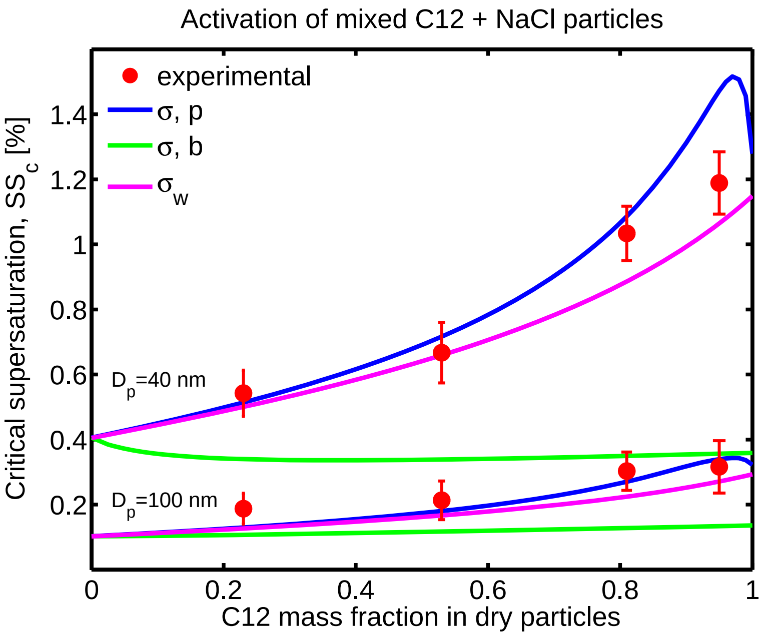

Fig. 4. Critical supersaturations (SS_c [%]) for particles with increasing mass fractions of sodium dodecanoate (w_{C12}), measured in experiments and modeled with the three different surfactant representations (σ,p, σ,b, and σ_w). Results are shown for selected dry particle sizes, D_p = 40 nm (upper curves and data points) and D_p = 100 nm (lower curves and data points).

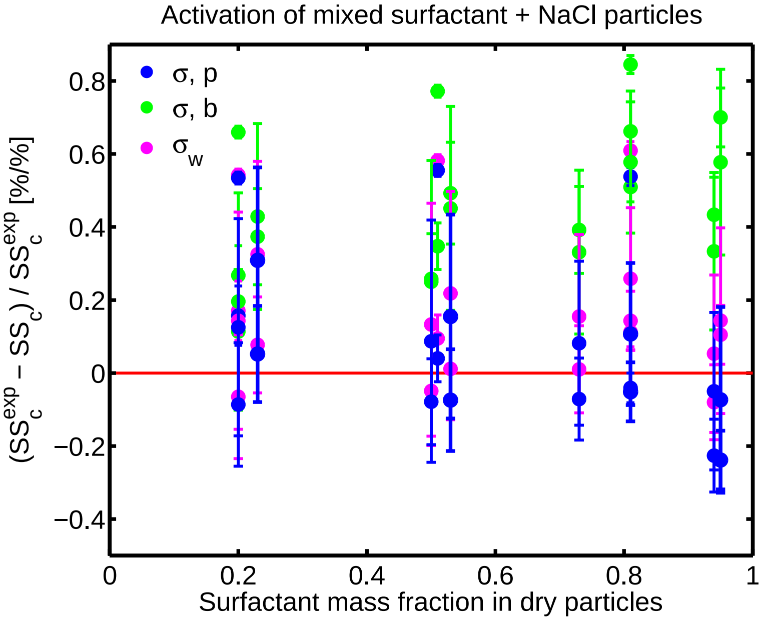

Fig. 5. Relative differences between experimental (SS_c^{exp} [%]) and modeled (SS_c [%]) critical supersaturations as a function of dry particle surfactant mass fraction (w_{SFT}). Results are shown for particles of all compositions studied, with selected dry sizes $D_p = 40$ and 100 nm.

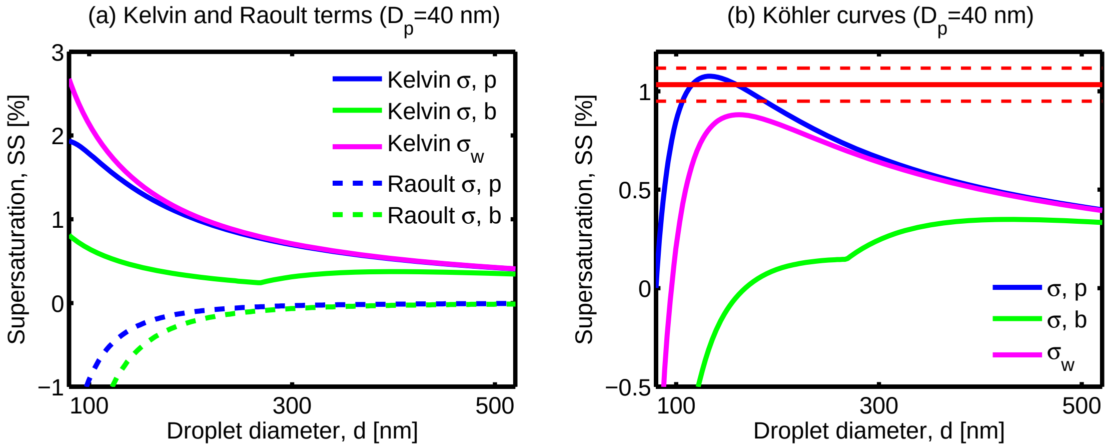

Fig. 6. Köhler model predictions with the different surfactant representations, for dry particles comprising 81% of C12 of diameter $D_p = 40$ nm: **(a)** individual Kelvin and Raoult contributions and **(b)** resulting Köhler curves. The experimental critical supersaturation SS_c^{exp} is depicted in panel (b) as a red line with corresponding 95%-confidence interval.

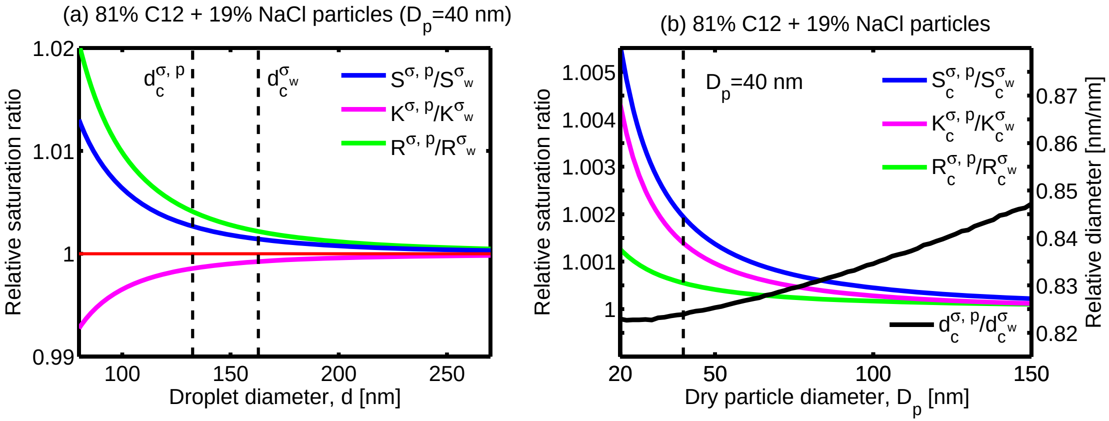

Fig. 7. Comparison of individual Kelvin (K) and Raoult (R) terms and resulting equilibrium saturation ratios (S) predicted with surfactant representations σ, p and σ_w for particles with 81% C12. Predictions are shown for growing droplets formed on 40 nm dry particles in panel **(a)** and at the respective points of droplet activation for particles of different dry sizes in panel **(b)**. The scale for the ratio of predicted critical droplet diameters in panel (b) is given on the right-hand y-axis.

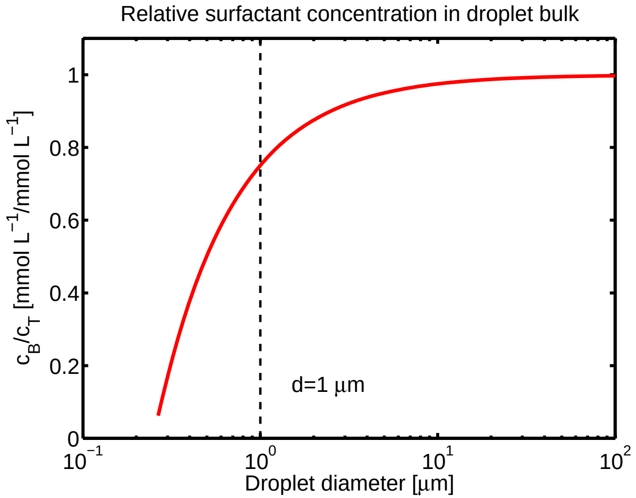

Fig. A1. Ratio of the surfactant bulk (c^B) and total (c^T) molarities as a function of droplet size (d). Droplets of all sizes have fixed total surfactant molarity $c^T = 40$ mmol L^{-1} and surfactant surface excess $\Gamma = 10^{18}$ m^{-2}.